

## DESIGN OF A COMPACT QUAD-BAND HYBRID ANTENNA FOR COMPASS/WiMAX/WLAN APPLICATIONS

Pan-Lin Shu and Quan-Yuan Feng\*

School of Information Science and Technology, Southwest Jiaotong University, Chengdu, Sichuan 610031, China

**Abstract**—A compact quad-band hybrid antenna for Compass/WiMAX/WLAN applications is proposed. The hybrid antenna is designed based on the method of combining a composite right/left-handed transmission line (CRLH-TL) unit cell with a meandered monopole and wide multi-band characteristics are achieved by merging some of resonance frequencies of the CRLH-TL unit cell and meandered monopole together. Coplanar waveguide (CPW) is used as a parallel excitation for both the CRLH-TL unit cell and meandered monopole. A prototype of the proposed hybrid antenna has been constructed and experimentally studied. The measured results show that four distinct operating bandwidths with 10 dB return loss are about 30 MHz (1.25–1.28 GHz), 290 MHz (2.44–2.73 GHz), 650 MHz (3.17–3.82 GHz) and 1130 MHz (5.03–6.16 GHz), covering the Compass B3, 2.5/3.5/5.5 GHz WiMAX and 5.2/5.8 GHz WLAN bands. Furthermore, the antenna has a single-layer planar structure with a small volume of only  $31 \times 21 \times 2 \text{ mm}^3$ . Acceptable radiation patterns and peak realized gains are obtained over the operating bands.

### 1. INTRODUCTION

With the blooming of modern wireless communication technologies, the demand for smaller wireless devices to work in different standards has increased significantly. Compact antennas with multi-band and wideband operations are vital for future wireless system [1]. Many kinds of multi-band antenna have been designed for the wireless local area network (WLAN) application in the 2.4 GHz (2.4–2.484 GHz)/5.2 GHz (5.15–5.35 GHz)/5.8 GHz (5.725–5.825 GHz)

---

*Received 27 February 2013, Accepted 27 March 2013, Scheduled 11 April 2013*

\* Corresponding author: Quan-Yuan Feng (fengquanyuan@163.com).

operating bands or the worldwide interoperability for microwave access (WiMAX) application in the 2.5 GHz (2.5–2.69 GHz)/3.5 GHz (3.3–3.8 GHz)/5.5 GHz (5.25–5.85 GHz) operating bands, such as monopole antenna with multiple resonance strips [2, 3] or parasitic elements [4, 5], slot antenna [6, 7], PIFA [8], fractal antenna [9], and dipole antenna [10–12], etc.. Although a great variety of studies about multiband antenna meeting the demands of WLAN or WiMAX applications have been reported, the subject about quad-band antenna for Compass B3 (1.256–1.278 GHz) or GPS, WiMAX and WLAN applications is seldom proposed. In [13], a paper-based inkjet-printed tri-band U-slot monopole antenna is proposed to cover the GPS/WiMAX/WLAN, but gain of the lowest frequency for GPS is only  $-6$  dBi. In [14] and [15], two slot antennas are presented to support quad-band operation for GPS/WiMAX/WLAN applications. But they also have the drawbacks of large size and complicated structures with double metallic layers.

The novel electromagnetic properties of metamaterials have been widely applied to RF device and antenna. Recently, there has been a great effort on miniaturized [16–18], multi-band [19–21] or leaky-wave [22–24] antennas based on the concept of metamaterials. Nevertheless, from the authors' point of view, the multi-band and/or multifunction antennas based on combination of the metamaterials and monopole antenna have not been fully explored. In this paper, a compact quad-band hybrid antenna for Compass/WLAN/WiMAX applications is proposed. The proposed antenna is implemented by combining a composite right/left-handed transmission line (CRLH-TL) unit cell with a meandered monopole and using coplanar waveguide (CPW) as its parallel excitation port. By carefully optimizing the gap width between radiating sections and CPW ground, length of the meandered monopole and dimensions of the CRLH-TL unit cell, preferable quad-band characteristics (1.25–1.28 GHz, 2.44–2.73 GHz, 3.17–3.82 GHz and 5.03–6.16 GHz) can be achieved. The proposed antenna also shows acceptable radiation characteristics and peak realized gains over the operating bands.

## 2. ANTENNA DESIGN AND SIMULATION

The geometry of the proposed compact quad-band hybrid antenna for Compass/WLAN/WiMAX applications is illustrated in Figure 1. The proposed antenna is printed on a low-cost FR4 substrate with thickness ( $h$ ) of 2 mm, relative permittivity ( $\epsilon_r$ ) of 4.4, and loss tangent of 0.02. The volume of the proposed antenna is only  $31 \times 21 \times 2$  mm<sup>3</sup>. The hybrid antenna is designed by combining a composite right/left-handed

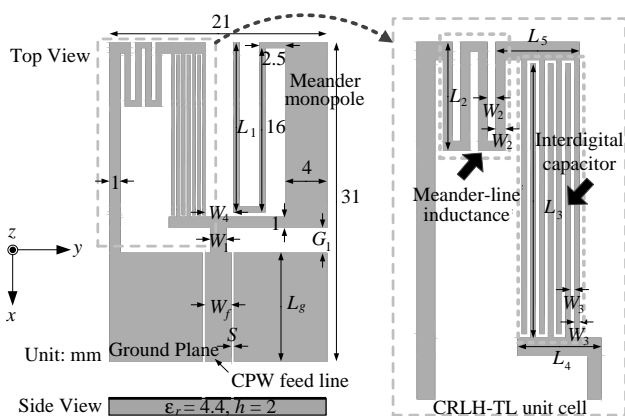


**Figure 1.** Geometry of the proposed CPW-fed quad-band hybrid antenna.

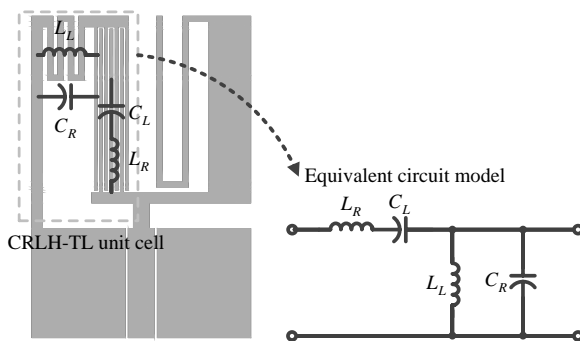


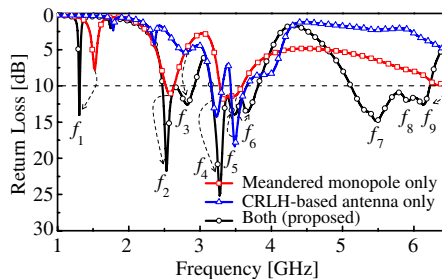
**Figure 2.** Equivalent circuit model of the CRLH-TL unit cell.

transmission line (CRLH-TL) unit cell with a meandered monopole. A  $50\ \Omega$  coplanar waveguide (CPW) is used as a parallel excitation for both the CRLH-TL unit cell and meandered monopole. The CPW feeding mechanism has a signal strip width of  $W_f = 2.5\text{ mm}$  and a gap distance of  $S = 0.3\text{ mm}$  between the signal strip and the CPW ground. As for the CRLH-TL unit cell, its equivalent circuit model is shown in Figure 2. The series capacitance ( $C_L$ ) has been implemented through an interdigital capacitor connected to the CPW feeding mechanism, while the shunt inductance ( $L_L$ ) has been obtained through a meandered-line strip placed between the interdigital capacitor (IDC) and the extended CPW ground. Moreover, the digits of the interdigital capacitor contribute the series inductance ( $L_R$ ), while the shunt capacitance ( $C_R$ ) can be found in the

coupling between the interdigital capacitor and the extended CPW ground as well as the spacing of the meandered lines. To maintain miniaturization, the meandered monopole is used with a total length of 62.5 mm, which corresponds to 0.26 wavelengths at 1.27 GHz.

For detailed design, Ansoft HFSS based on finite element method (FEM) has been employed to analyze and optimize the electrical properties and radiation characteristics of the antenna. Via iterative design process, the proper parameters for optimal quad-band operation of the proposed antenna are set as follows:  $G_1 = 2.5$  mm,  $W_1 = 1.5$  mm,  $W_2 = 0.5$  mm,  $W_3 = 0.25$  mm,  $W_4 = 2.75$  mm,  $L_1 = 16.5$  mm,  $L_2 = 6.2$  mm,  $L_3 = 15.75$  mm,  $L_4 = 4.75$  mm,  $L_5 = 4.75$  mm,  $L_g = 10.5$  mm.

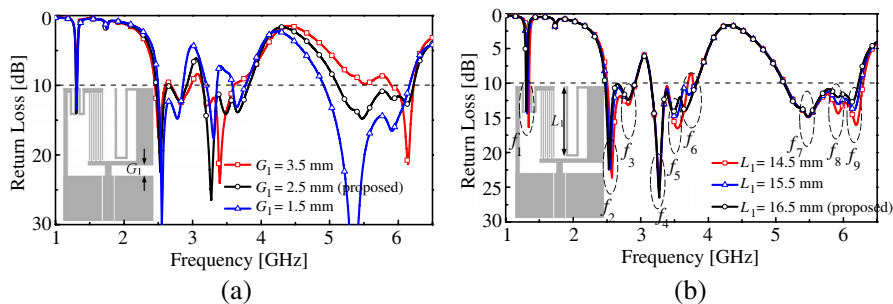
Figure 3 shows a comparison of the simulated return losses for the proposed hybrid antenna, the case with the meandered monopole antenna only, and the case with the CRLH-TL based antenna only. Results clearly show that the CRLH-TL based antenna generates two narrow operating bands resonated at 3.2/3.5 GHz with a poor impedance matching resonant frequency at 2.8 GHz. Analogously, the meandered monopole antenna generates four narrow operating bands resonated at 1.5/2.55/3.45/6.4 GHz. The bandwidths of the two cases are too narrow to meet the requirements of practical applications. However, with the combination of the CRLH-TL unit cell and the meandered monopole, a quad-band hybrid antenna is achieved. The CRLH-TL unit cell and meandered monopole share the same CPW feeding mechanism (see Figure 1). The resonant frequencies of the proposed hybrid antenna are named of  $f_1, f_2 \dots f_9$ , respectively, as shown in Figure 3. And dotted arrows are used to mark the corresponding relationships between  $f_1, f_2 \dots f_6, f_9$  and the resonant frequencies generated by the meandered monopole antenna



**Figure 3.** Comparison of the simulated return losses for the proposed hybrid antenna, the case with the meandered monopole antenna only, and the case with the CRLH-based antenna only.

only and the CRLH-TL based antenna only. For example, the resonant frequency of the proposed hybrid antenna at  $f_2$  corresponds to the one at 2.55 GHz generated by the meandered monopole antenna only. It can be obviously observed that the hybrid antenna merges both the resonant frequencies of CRLH-TL unit cell and meandered monopole together to generate three wide operating bands, ranging from 2.47 to 2.92 GHz ( $f_2$  and  $f_3$ ), 3.16 to 3.83 GHz ( $f_4$ ,  $f_5$  and  $f_6$ ), and 5.11 to 6.23 GHz ( $f_7$ ,  $f_8$  and  $f_9$ ). The three wide operating bands cover 2.5/3.5/5.5 GHz WiMAX and 5.2/5.8 GHz WLAN applications. Because of electromagnetic coupling between the CRLH-TL unit cell and the meandered monopole, the lowest resonant frequency (1.5 GHz) of the meandered monopole antenna shifts down to  $f_1 = 1.27$  GHz to satisfy the demand of Compass B3 operating bands. In this case, the quad-band hybrid antenna for Compass B3, 2.5/3.5/5.5 GHz WiMAX and 5.2/5.8 GHz WLAN applications is obtained.

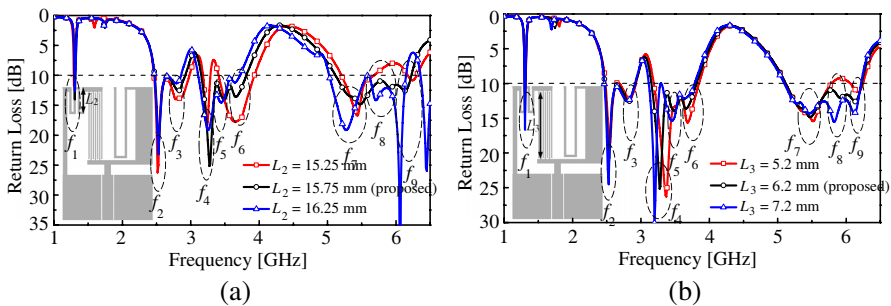
The gap  $G_1$  between the radiating sections and CPW ground is a critical parameter to control the impedance bandwidth, as shown in Figure 4(a). Clearly, as the decrease of  $G_1$ , the bandwidths of the second and third band tend to be narrow, but the last one becomes wide with improved impedance matching. For covering the desired quad-band operation,  $G_1$  is selected to be 2.5 mm in this study. Figure 4(b) shows the results of the simulated return losses as a function of the length of meandered monopole  $L_1$ . As expected,  $L_1$  mainly affects the operating frequencies  $f_1$ ,  $f_2$ ,  $f_6$  and  $f_9$  generated by the meandered monopole. As the decrease of  $G_1$ , all the operating frequencies  $f_1$ ,  $f_2$ ,  $f_6$  and  $f_9$  shift toward the higher frequency. The operating frequency at  $f_1$  is the meandered monopole's quarter-wave mode and the other operating frequencies at  $f_2$ ,  $f_6$  and  $f_9$  are the meandered monopole's



**Figure 4.** Simulated return losses of the proposed antenna with different (a) gap width  $G_1$  and (b) the length of meandered monopole  $L_1$ .

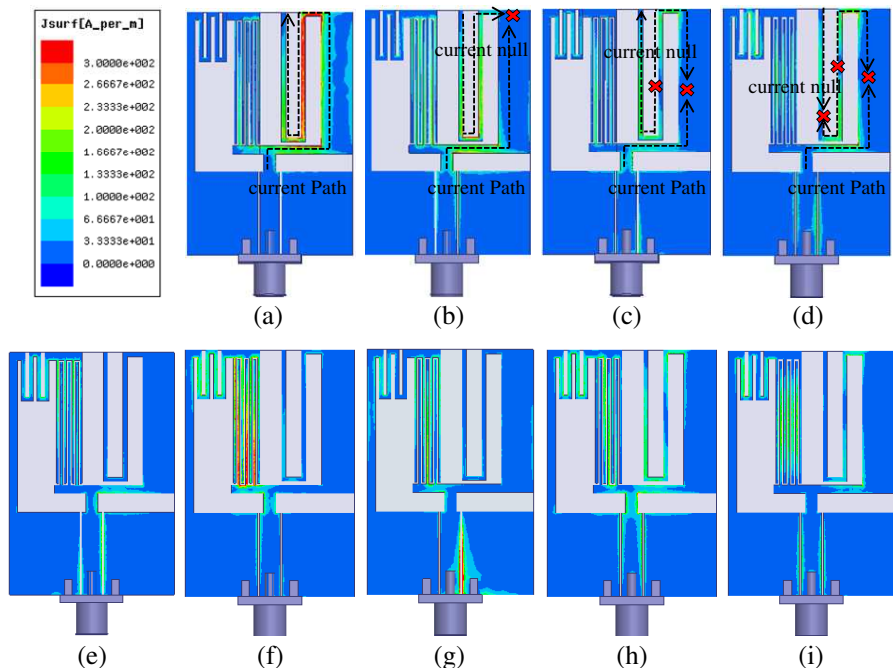
higher order modes. In order to meet the application of Compass B3 operating band (1.258–1.278 GHz), the optimal value of  $L_1$  is 16.5 mm.

Figure 5 shows the results of the simulated return losses of the proposed antenna with different parameters of the CRLH-TL unit cell. As expected,  $L_2$  and  $L_3$  mainly affect the operating frequencies  $f_3$ ,  $f_4$  and  $f_5$  generated by different parts of the CRLH-TL unit cell and also have a great effect on  $f_7$ ,  $f_8$  and  $f_9$ . With the increase of the parameters  $L_2$  and  $L_3$ , all the operating frequencies  $f_3$ ,  $f_4$ ,  $f_5$ ,  $f_7$ ,  $f_8$  and  $f_9$  shift toward the lower frequency. Results show that when the length  $L_2$  and  $L_3$  are chosen to be 6.2 mm and 15.75 mm, respectively, preferable quad-band characteristics with good impedance matching for Compass B3, 2.5/3.5/5.5 GHz WiMAX and 5.2/5.8 GHz WLAN applications are achieved for the proposed hybrid antenna.



**Figure 5.** Simulated return losses of the proposed antenna with different parameters of the CRLH-TL unit cell (a)  $L_2$  and (b)  $L_3$ .

In order to further demonstrate the operation mechanism, surface current distributions on the whole proposed antenna at the resonant frequencies are shown in Figure 6. It can be clearly seen that the current has different distributions along the antenna in different resonant frequencies. In Figures 6(a)–(d), the surface currents are mainly concentrated at the meandered monopole. It confirms that the resonant frequencies at  $f_1$ ,  $f_2$ ,  $f_6$  and  $f_9$  are excited by the meandered monopole. Furthermore, from the current path in Figure 6(a), it can be seen that fundamental mode (quarter-wave mode) of the meandered monopole at  $f_1$  is excited with a 0.26 wavelengths current length. In Figures 6(b)–(d), there is at least one current null in the meandered monopole, which confirms that the resonant frequencies at  $f_2$ ,  $f_6$  and  $f_9$  are the higher-order mode excited by the meandered monopole. In Figures 6(e)–(g), the surface currents are mainly concentrated at the different parts of the CRLH-TL unit cell. It confirms that the resonant frequencies at  $f_3$ ,  $f_4$  and  $f_5$  are excited by different parts of the CRLH-



**Figure 6.** Simulated surface current distributions of the proposed antenna at (a)  $f_1 = 1.27$  GHz, (b)  $f_2 = 2.53$  GHz, (c)  $f_6 = 3.66$  GHz, (d)  $f_9 = 6.13$  GHz, (e)  $f_3 = 2.82$  GHz, (f)  $f_4 = 3.29$  GHz, (g)  $f_5 = 3.49$  GHz, (h)  $f_7 = 5.48$  GHz, (i)  $f_8 = 5.91$  GHz.

TL unit cell. In Figures 6(h)–(i), the surface currents are distributed at both the meandered monopole and the CRLH-TL unit cell, indicating that electromagnetic coupling between the meandered monopole and the CRLH-TL unit cell generate the resonances at  $f_7$  and  $f_8$ .

### 3. EXPERIMENTAL RESULTS AND DISCUSSION

A fabricated prototype of the proposed quad-band hybrid antenna has been experimentally studied, as depicted in Figure 7. As the CRLH-TL unit cell, meandered monopole and CPW feeding mechanism are implemented on the same plane, fabrication of the proposed antenna is very easy to use a single-layer metallization process. The return loss of the proposed hybrid antenna was measured with Agilent E5071C ENA network analyzer. The measured and simulated return losses against frequency for the proposed antenna are presented in Figure 8.

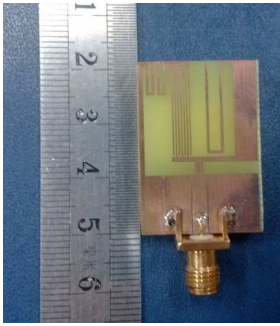


**Figure 7.** Photograph of the fabricated quad-band hybrid antenna.

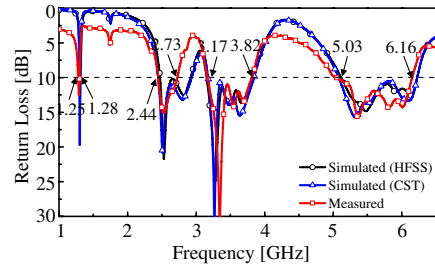


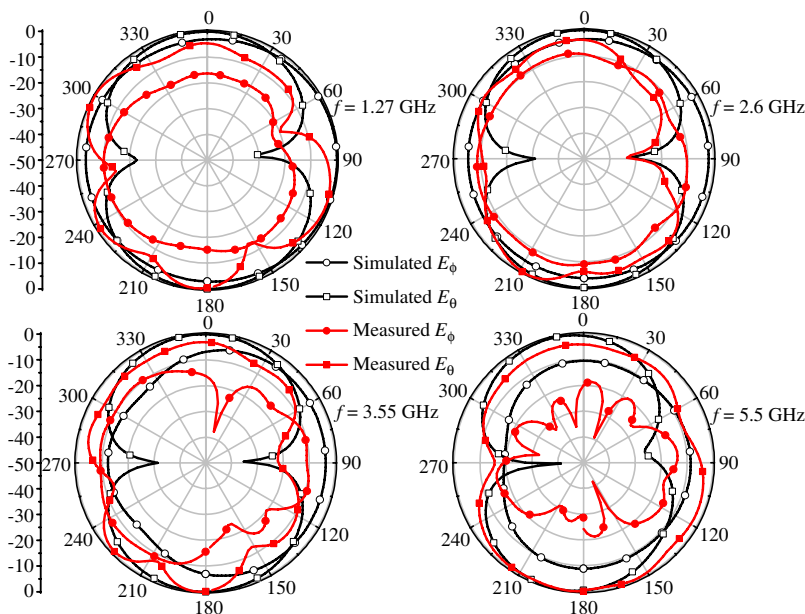
**Figure 8.** Measured and simulated return losses for the proposed antenna.

From the measured results, four distinct operating bandwidths with 10 dB return loss are about 30 MHz (1.25–1.28 GHz), 290 MHz (2.44–2.73 GHz), 650 MHz (3.17–3.82 GHz) and 1130 MHz (5.03–6.16 GHz), corresponding to an impedance bandwidth of 2.4%, 11.2%, 18.6% and 20.2% with respect to the center frequency, respectively. And it is easy to cover the required bandwidths for Compass B3, 2.5/3.5/5.5 GHz WiMAX and 5.2/5.8 GHz WLAN bands. Good agreement between the simulation and measurement can be observed, although the second operating band is narrow than the simulated result. However, the reasons attributed to the differences are believed 1) the manufacturing tolerances about the related pivotal physical parameters, such as  $S$ ,  $W_2$  and  $W_3$ ; 2) the uncertainty of the dielectric constant of the FR4 substrate, ranging from 4.2 to 4.6; and 3) the coupling between the SMA connector and various parts of the antenna.

The radiation patterns of the proposed hybrid antenna were measured in a SATIMO StarLab microwave anechoic chamber. Figure 9 shows the measured and simulated far-field normalized radiation patterns in the  $E$ -plane ( $x$ - $z$  plane) and  $H$ -plane ( $y$ - $z$  plane) of the proposed antenna. For the  $E$ -plane, the co-polarization component corresponds to  $E_\theta$ , whereas the cross-polarization one corresponds to  $E_\varphi$ ; for the  $H$ -plane, the co-polarization component corresponds to  $E_\varphi$ , and the cross-polarization one corresponds to  $E_\theta$ . As expected,  $H$ -plane tends to be omnidirectional, whereas  $E$ -plane shows the monopole-like pattern. The  $y$ -directed currents along the horizontal sections of the meandered-line strip and the meandered monopole have a contribution to the cross-polarization in the  $E$ -plane, which make the co- and cross-polarization components have comparable magnitude, especially at 1.27 GHz, 2.6 GHz and

3.55 GHz. Nevertheless, this radiation characteristic is still acceptable because in modern wireless communications, the orientation of the handset or portable computer is not fixed, and the incoming signals are depolarized due to multiple reflections and scattering in the propagation channel. It is, therefore, important that the antenna should be capable of receiving both the co- and cross-polarization components [25]. A good agreement between the measured and simulated radiation patterns are observed, especially in  $H$ -plane. The slight differences are mainly due to the spurious reflections from RF cable that is not incorporated in the simulation. Having taken the impedance mismatch into account, the measured and simulated peak realized gains of the proposed antenna are depicted in Figure 10. The measured minimum gains in the operating bands of 1.25–1.28 GHz, 2.5–2.7 GHz, 3.3–3.8 GHz and 5.15–5.85 GHz are  $-4.88$  dBi, 2.82 dBi, 1.84 dBi and 1.78 dBi, respectively. Due to large dielectric loss of the FR4 substrate at high frequencies, the measured gains in the last band are relatively small compared with the simulated results. However, the gains of the proposed antenna still satisfy the requirement of some actual applications.

The performances of the proposed antenna are compared with those of the recently reported antennas [13–15, 26] for the Compass



(a)

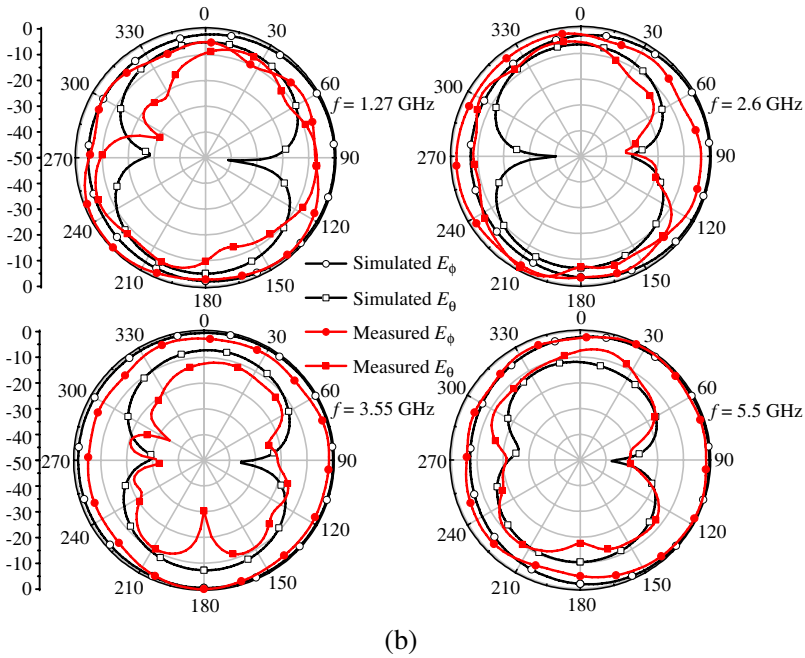


**Figure 9.** Measured and simulated normalized radiation patterns at 1.27, 2.6, 3.55, and 5.5 GHz in (a)  $E$ -plane ( $x$ - $z$  plane) and (b)  $H$ -plane ( $y$ - $z$  plane).

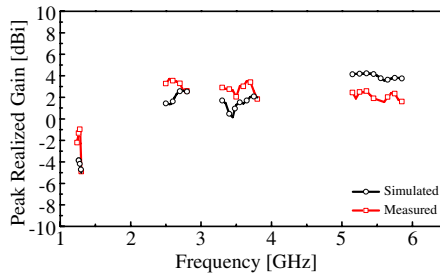


**Figure 10.** Measured and simulated peak realized gains.

or GPS, WLAN and WiMAX applications in Table 1. Although the proposed antenna is realized with a relatively compact size, it still provides competitively enhanced bandwidths covering the Compass B3, 2.5/3.5/5.5 GHz WiMAX and 5.2/5.8 GHz WLAN bands. The gain of the first mode (resonant frequency) is larger than reference [13] and [15]. Moreover, it is easy to be fabricated and low cost owing

**Table 1.** Comparison results of the proposed and reference antennas.

Reference	Proposed	[13]	[14]	[15]	[26]
Size (mm <sup>3</sup> )	31 × 21 ×2	40 × 38 ×0.44	36 × 42 ×1	60 × 53 ×0.8	30 × 30 ×1.6
Layer	Single	Double	Double	Double	Single
Operating bands (GHz)	1.25–1.28 2.44–2.73 3.17–3.82 5.03–6.16	1.53–1.58 2.75–3.65 4.25–6.12	1.54–1.70 2.38–2.76 3.20–3.77 5.12–6.25	1.515–1.625 2.332–2.495 3.42–3.70 5.05–5.94	1.17–1.58 2.40–2.70 3.40–3.69 4.70–5.50
Gain of the first mode (dBi)	−0.88	−6	1.84	−1	0.507

to the single-layer. Because of the appropriate return loss in the four operating bands and acceptable far-field characteristics, the proposed antenna is suitable for Compass, WiMAX and WLAN wireless communication system applications.

#### 4. CONCLUSION

A compact CPW-fed quad-band hybrid antenna has been presented and studied. By combining the CRLH-TL unit cell with a meandered monopole, four distinct operating bands which can meet the requirements for Compass B3, 5.2/5.8 GHz WLAN and 2.5/3.5/5.5 GHz WiMAX applications are obtained, ranging from 1.25–1.28 GHz, 2.44–2.73 GHz, 3.17–3.82 GHz and 5.03–6.16 GHz, respectively. The proposed antenna has the advantages of easy fabrication, low cost, and compact size, showing good quad-band operating bandwidths and acceptable radiation characteristics. Consequently, the proposed antenna is expected to be a good candidate for Compass/WiMAX/WLAN wireless communication systems.

#### ACKNOWLEDGMENT

This work is supported by the National Natural Science Foundation of China (NNSF) under Grant 60990320, 60990323, 61271090, and the National 863 Project of China under Grant 2012AA012305, and Sichuan Provincial Science and technology support Project under

Grant 2012GZ0101, and Chengdu Science and technology support Project under Grant 12DXYB347JH-002.

## REFERENCES

1. Luk, K. M., "The importance of the new developments in antennas for wireless communications," *Proceedings of the IEEE*, Vol. 99, 2082–2084, 2011.
2. Panda, J. R. and R. S. Kshetrimayum, "A printed 2.4 GHz/5.8 GHz dual-band monopole antenna with a protruding stub in the ground plane for WLAN and RFID applications," *Progress In Electromagnetics Research*, Vol. 117, 425–434, 2011.
3. Lu, J.-H. and Y.-H. Li, "Planar multi-band T-shaped monopole antenna with a pair of mirrored L-shaped strips for WLAN/WiMAX operation," *Progress In Electromagnetics Research C*, Vol. 21, 33–44, 2011.
4. Shu, P. and Q. Feng, "Compact tri-band monopole antenna with a parasitic E-shaped strip for WLAN/WiMAX applications," *Progress In Electromagnetics Research C*, Vol. 32, 53–63, 2012.
5. Sayidmarie, K. H. and T. A. Nagem, "Compact dual-band dual-ring printed monopole antennas for WLAN applications," *Progress In Electromagnetics Research B*, Vol. 43, 313–331, 2012.
6. Wang, C.-J. and S.-W. Chang, "Studies on dual-band multi-slot antennas," *Progress In Electromagnetics Research*, Vol. 83, 293–306, 2008.
7. Ren, F.-C., F.-S. Zhang, B. Chen, Y.-T. Wan, and Y.-C. Jiao, "Compact triple-band slot antenna for wireless communications," *Progress In Electromagnetics Research Letters*, Vol. 31, 89–96, 2012.
8. Wang, H. and M. Zheng, "An internal triple-band WLAN antenna," *IEEE Antennas and Wireless Propagation Letters*, Vol. 10, 569–572, 2011.
9. Li, D., F.-S. Zhang, Z.-N. Zhao, L.-T. Ma, and X. N. Li, "A compact CPW-FED Koch snowflake fractal antenna for WLAN/WiMAX applications," *Progress In Electromagnetics Research C*, Vol. 28, 143–153, 2012.
10. Ku, C.-H. and H.-W. Liu, "Compact planar triple-band folded dipole antenna for WLAN/WiMAX applications," *Progress In Electromagnetics Research C*, Vol. 28, 1–13, 2012.
11. Guo, Y. Y., X.-M. Zhang, G.-L. Ning, D. Zhao, X. W. Dai, and Q. Wu, "Miniaturized modified dipoles antenna for WLAN

- applications,” *Progress In Electromagnetics Research Letters*, Vol. 24, 139–147, 2011.
12. Li, D. and J.-F. Mao, “Koch-like sided Sierpinski Gasket multifractal dipole antenna,” *Progress In Electromagnetics Research*, Vol. 126, 399–427, 2012.
  13. AbuTarboush, H. and A. Shamim, “Paper-based inkjet printed tri-band U-slot monopole antenna for wireless applications,” *IEEE Antennas and Wireless Propagation Letters*, Vol. 11, 1234–1237, 2012.
  14. Xiong, L., P. Gao, and P. Tang, “Quad-band rectangular wide-slot antenna for GPS/WiMAX/WLAN applications,” *Progress In Electromagnetics Research C*, Vol. 30, 201–211, 2012.
  15. Sun, X., G. Zeng, H.-C. Yang, Y. Li, X.-J. Liao, and L. Wang, “Design of an edge-FED quad-band slot antenna for GPS/WiMAX/WLAN applications,” *Progress In Electromagnetics Research Letters*, Vol. 28, 111–120, 2012.
  16. Jang, T., J. Choi, and S. Lim, “Compact coplanar waveguide (CPW)-FED zeroth-order resonant antennas with extended bandwidth and high efficiency on vialess single layer,” *IEEE Transactions on Antennas and Propagation*, Vol. 59, 363–372, 2011.
  17. Liu, X., S. N. Burokur, A. de Lustrac, G. Sabanowski, and G. P. Piau, “Compact base station antennas using metamaterials,” *Progress In Electromagnetics Research C*, Vol. 33, 43–53, 2012.
  18. Yu, H. Z. and Q. X. Chu, “An omnidirectional small loop antenna based on first-negative-order resonance,” *Journal of Electromagnetic Waves and Applications*, Vol. 26, No. 1, 111–119, 2012.
  19. Du, G.-H., X. Tang, and F. Xiao, “Tri-band metamaterial-inspired monopole antenna with modified S-shaped resonator,” *Progress In Electromagnetics Research Letters*, Vol. 23, 39–48, 2011.
  20. Liu, S.-X. and Q. Feng, “Compact multi-band loop antennas using CPW-based CRLH quarter-wave type resonators,” *Progress In Electromagnetics Research C*, Vol. 28, 47–60, 2012.
  21. Ibrahim, A. and A. Safwat, “Microstrip-fed monopole antennas loaded with CRLH unit cells,” *IEEE Transactions on Antennas and Propagation*, Vol. 60, 4027–4036, 2012.
  22. Mujumdar, M. D., J. Cheng, and A. Alphones, “Double periodic composite right/left handed transmission line based leaky wave antenna by singular perturbation method,” *Progress In Electromagnetics Research*, Vol. 132, 113–128, 2012.

23. Geng, L., G.-M. Wang, H.-Y. Zeng, and M.-W. Chui, "Dual composite right/left-handed leaky-wave structure for dual-polarized antenna application," *Progress In Electromagnetics Research Letters*, Vol. 35, 191–199, 2012.
24. Anghel, A. and R. Cacoveanu, "Improved composite right/left-handed cell for leaky-wave antenna," *Progress In Electromagnetics Research Letters*, Vol. 22, 59–69, 2011.
25. Sun, X., G. Zeng, H.-C. Yang, and Y. Li, "Compact quadband CPW-FED slot antenna for M-WiMAX/WLAN applications," *IEEE Antennas and Wireless Propagation Letters*, Vol. 11, 395–398, 2012.
26. Lin, C. P., C. H. Chang, and C. F. Jou, "Compact quad band monopole antenna," *Microwave and Optical Technology Letters*, Vol. 53, 1272–1276, 2011.